

LASERS AND AMPLIFIERS

PACS numbers: 42.55.Px; 42.60.Jf
DOI: 10.1070/QE2001v031n10ABEH002061

Dependence of the radiation pattern of a leaky-mode, quantum-well heterolaser on the pump current

A P Bogatov, A E Drakin, A A Lyakh, A A Stratonnikov

Abstract. **The dependences of the angular position and angular width of peaks in the far-field zone of a leaky-mode laser on the pump current are studied. It is found that an increase in the concentration of carriers in active layers results in a deviation of a laser beam with respect to the normal to the diode-laser facet and in a decrease in the beam divergence, while an increase in the temperature of waveguide layers compared to a substrate reduces the angle between the beam axis and the normal to the laser mirror.**

Keywords: *heterolasers, radiation pattern, leaky modes.*

1. Introduction

Semiconductor lasers and optical amplifiers based on heterostructures representing a waveguide with radiation leaking to a substrate can be considered as one of the possible types of a powerful and efficient optical radiator [1 – 3]. The radiation leakage occurs due to radiation tunnelling from waveguide layers through one of the cladding layers to a transparent substrate. The tunnelled radiation propagates over the substrate as an inhomogeneous plane wave, which forms a collimated beam in the far-field zone of the laser radiation. In this way, the laser radiation is extracted over the entire length of the resonator.

Compared to the common design of a semiconductor laser, this design promise the obtaining of higher output powers due to a decrease in the optical load at the output mirror, as well as a substantial decrease (an order of magnitude and more) in the width of the radiation pattern.

Because the radiation pattern is one of the basic characteristics of any semiconductor laser, its dependence on the pump current is of interest and is studied in this paper.

We paid main attention to changes in the angular positions of peaks in the far-field pattern and the dependence of their width on the pump current of the diode laser.

A P Bogatov, A E Drakin P N Lebedev Physics Institute, Russian Academy of Sciences, Leninsky prosp. 53, 119991 Moscow, Russia
A A Lyakh, A A Stratonnikov Moscow Institute of Physics and Technology (State University), Institutskii per. 9, 141700 Dolgoprudnyi, Moscow oblast', Russia

Received 24 July 2001
Kvantovaya Elektronika **31** (10) 847 – 852 (2001)
Translated by M N Sapozhnikov

2. Experiment

We used lasers based on one of the heterostructures InGaAs/AlGaAs/GaAs and emitting at a wavelength of 0.98 μm. The parameters of such lasers are presented in paper [3]. Some characteristics of this heterostucture are presented in Table 1. We studied two samples with the resonator length of 400 μm, two samples with the resonator length of 600 μm, and one sample with the resonator length of 1200 μm. The radiation pattern was detected using a computer-controlled automated setup. The setup, which is described in detail in paper [4], provided the scan of the radiation pattern with an angular resolution of $\sim 0.1^\circ$. The position θ_m of the maxima and the width $\Delta\theta$ of the angular intensity distribution in the far-field zone were determined by the method of least squares using the model dependence

$$I(\theta) = A + B\left[1 + \frac{(\theta - \theta_m)^2}{\Delta\theta^2}\right]^{-1}.$$

Table 1. Properties of heterostructures studied.

Layer number	Layer	Layer composition (assumed)	Refractive index	Layer thickness/μm
1		*p*-GaAs:Zn	3.52	0.3
2		*p*-GaAs:Zn	3.52	0.2
3	Cladding	$Al_{0.41}Ga_{0.59}As$	3.28	0.7
4	Waveguide	GaAs	3.51	0.59
5		$Al_{0.15}Ga_{0.85}As$	3.435	0.05
6	Active	$In_{0.2}Ga_{0.8}As$	3.2	0.008
7		$Al_{0.15}Ga_{0.85}As$	3.435	0.05
8	Active	$In_{0.2}Ga_{0.8}As$	3.2	0.008
9		$Al_{0.15}Ga_{0.85}As$	3.435	0.05
10	Waveguide	GaAs	3.51	0.3
11	Cladding	$Al_{0.41}Ga_{0.59}As$	3.36	0.34
12		*n*-GaAs:Si	3.51	0.42
13		*n*-GaAs:Si	3.51	300

The measurements were performed at room temperature using repetitively pulsed pumping by 300-ns pulses with a repetition rate of 1 kHz. Fig. 1 shows the typical light – current characteristic and the radiation pattern for the samples in the direction perpendicular to the structure layers. Hereafter, we present the results obtained for 'a short' sample of length 400 μm. The behaviour of another sample of the same length was qualitatively identical. The threshold current density and the differential efficiency estimated from the light – current characteristic are 6 kA cm^{-2} and 0.5 W A^{-1}, respec-

tively. Note that these values had a substantial scatter both for samples made of different heterostructures and for different samples made of the same heterostructure. However, the efficiency, as a rule, did not exceed 0.5 W A^{-1}, while the scatter of threshold currents was from 0.6 to 6 kA cm^{-2}.

The radiation pattern presented in Fig. 1 (the pump current density was 10 kA cm^{-2}) exhibits the features typical for leaky-mode lasers. A broad band is observed with a maximum near zero, which is formed by the fraction of radiation localised in waveguide layers. The basic feature is the presence of two narrow peaks at 30° and 47°, which corresponds to the leaking radiation in the zero and first transverse modes of the waveguide.

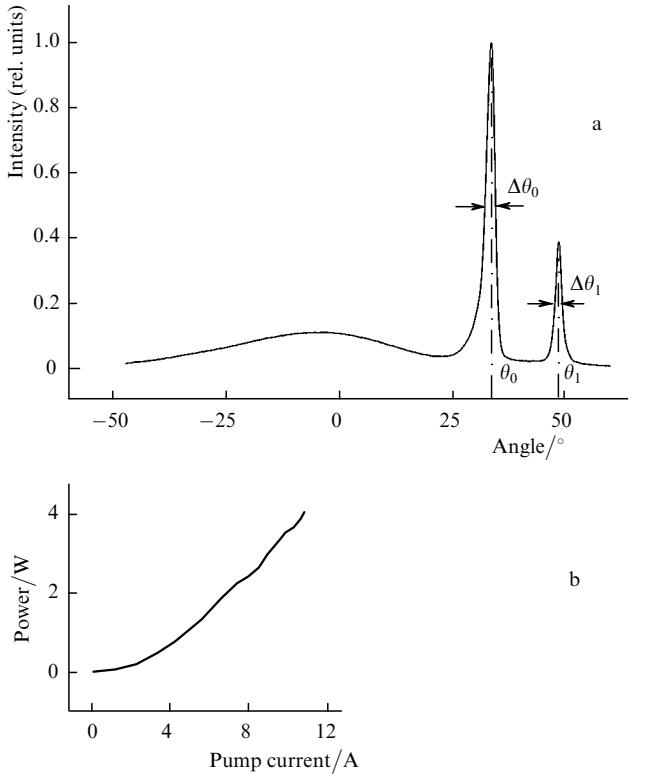

Figure 1. Typical radiation pattern of samples in a plane perpendicular to the structure layers (the positions θ_0 and θ_1 and widths $\Delta\theta_0$ and $\Delta\theta_1$ of peaks corresponding to the zero and first leaky modes, respectively, are shown) (a) and a typical light–current characteristic of samples (b). The differential efficiency is approximately 0.5 W A^{-1}.

The generation on the first transverse mode was observed not for all samples studied. This probably depends on the relation between the threshold gain and losses for the zero and the first transverse modes. The results presented below were obtained for samples in which along with the zero mode the first mode could be also excited. As a rule, these samples had a smaller resonator length and a higher threshold current density compared to other samples studied. In particular, no generation at the first mode was observed in lasers with the resonator length ~ 1200 μm and the threshold current density ~ 0.6 kA cm^{-2}.

Fig. 2 shows the radiation pattern calculated for the model waveguide structure, which is more close, in our opinion, to the structure from which the samples were manufactured (the degree of the correspondence will be discussed below). One can see that the calculated and experimental angular positions of the first mode peak well coincide. In addition, the calculated and experimental radiation patterns for the zero mode peak and for the contour corresponding to radiation from the region of waveguide layers are also in good agreement. These calculations do not reflect the relation between the intensities upon lasing but correspond to spontaneous radiation.

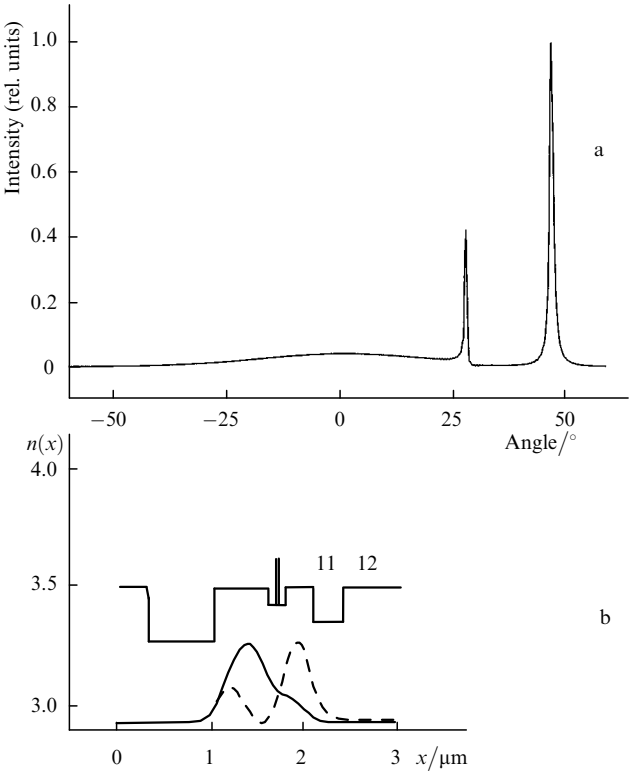

Figure 2. Model radiation pattern in a plane perpendicular to the structure layers (a) and the model profile of the refractive index of the waveguide and the calculated distribution of the radiation intensity in the waveguide for the zero (solid curve) and first (dashed curve) modes (b). A noticeable leaking of the first mode through facing layer 11 to substrate 12 is seen.

Because the angular positions θ_0 and θ_1 of the peaks are completely determined by the effective waveguide value of the refractive index of the mode [3], it is expedient to study their dependence on the pumping current. These data are presented in Fig. 3. One can see that the angles θ_0 and θ_1 increase with pump current below the lasing threshold and decrease above the threshold.

Note that, unlike conventional lasers, the lasers studied here exhibit a distinct characteristic mode structure (peaks) in the far field below the threshold [4]. This circumstance was used in paper [4] for the experimental measurement of the spontaneous radiation factor. One can see from curves in Fig. 3 that not only the sign of the change in θ_0 and θ_1 with the pump current is different below and above the threshold, but also the magnitude of the rate of this change. The processing of these data shows that for $j < j_{th}$ the derivative $d\theta_0/dj$ is larger that $d\theta_1/dj$ by a factor of 1.6, whereas for $j > j_{th}$ these derivatives become negative and have close values.

Our experiments showed that along with the change in the angular positions of the peaks in the far field, their half-widths $\Delta\theta_0$ and $\Delta\theta_1$ also change. The half-widths of the zero

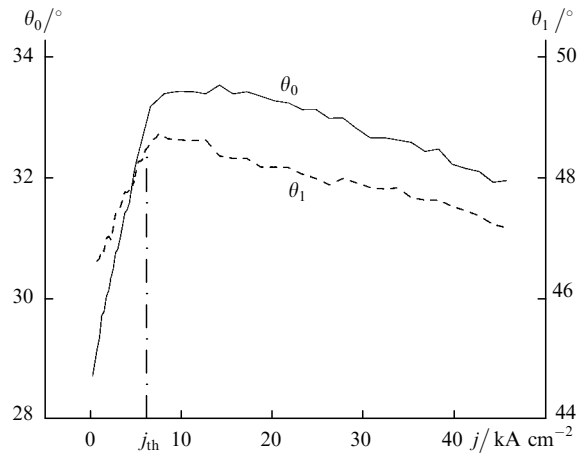

Figure 3. Dependences of the positions θ_0 and θ_1 of the peaks of the zero and first leaky modes, respectively, on the pump current density. Below the threshold j_{th}, the leakage angle increases with current, while above the threshold, it decreases.

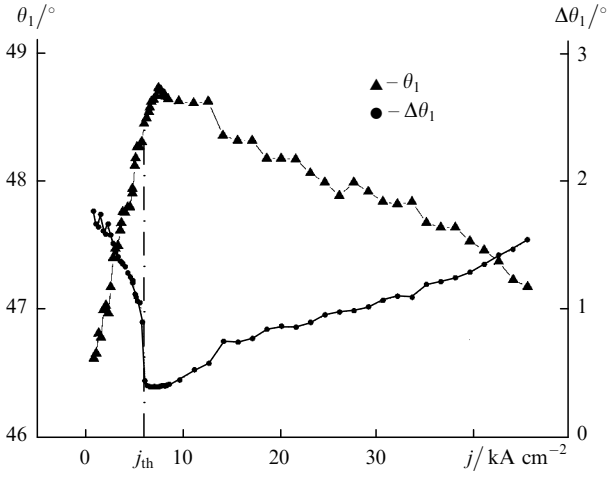

Figure 4. Dependence of the width $\Delta\theta_1$ of the peak of the first leaky mode on the pump current density. For comparison, the peak position θ_1 is also shown.

and first modes changes qualitatively in the same way. Fig. 4 shows the dependence of $\Delta\theta_1$ on the pumping current density for the first mode, as well as such dependence for the angle θ_1 itself for the same sample. One can see that the value of $\Delta\theta_1$ sharply decreases with the pump current density below the threshold and slowly increases above the threshold.

Fig. 5 shows the relative distribution of the output power in the peaks corresponding to the zero and first modes in the far-field zone of the laser. Lasing first occurs at the zero mode, and then lasing at the first mode develops with increasing pump current. Because we did not study the lasing dynamics in our experiments, the data presented in Fig. 5 do not allow us to interpret unambiguously the 'instant' distribution of the output power over the modes. Thus, it is not inconceivable that lasing can switch from one mode to another during the pulse. In any case, the presented data demonstrate a 'mean' (during the pulse) distribution of the output power among the zero and first transverse modes.

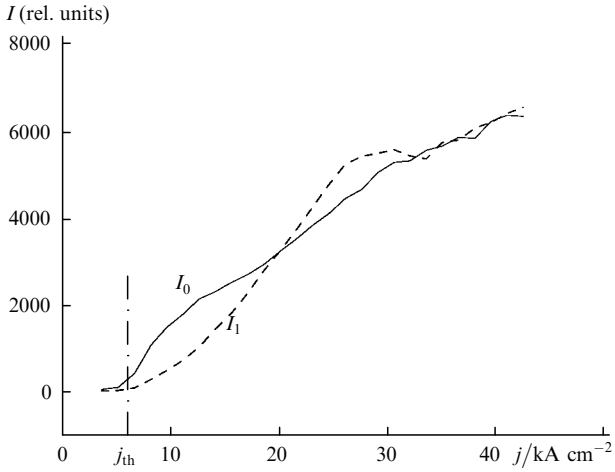

Figure 5. Dependences of the relative radiation intensities I_0 and I_1 of the zero and first leaky modes, respectively, on the pump current density.

Going to the discussion of the results of measurements, we should bear in mind that the absolute changes $\delta\theta_0$ and $\delta\theta_1$ in the angles θ_0 and θ_1 upon varying the pump current are $\sim 2^\circ$ (see Fig. 3), which is not very large compared to the half-widths $\Delta\theta_0$ and $\Delta\theta_1$ of the peaks. In the best case, the changes $\delta\theta_0$ and $\delta\theta_1$ in the angles over the entire pumping range exceed the minimum widths $\Delta\theta_0$ and $\Delta\theta_1$ ($\sim 0.4^\circ$) of the peaks only by a factor of three. In the worst case (the broadest peaks at the minimum and maximum pump currents), the values of $\Delta\theta_0$ and $\Delta\theta_1$ are comparable with $\delta\theta_0$ and $\delta\theta_1$. Nevertheless, we can state with confidence that the data presented in Figs 3 and 4 are correct. This is confirmed, first, by a comparatively small scatter of points in plots $\theta_0(j)$ and $\theta_1(j)$ and, second, by a sufficiently high reproducibility of the results obtained for the same sample and by the similarity of the radiation patterns obtained for other samples under close experimental conditions. This was achieved due to the automation of experiments with the help of a PC with the digital data recording and processing.

3. Discussion of the results

Our study showed that the values of the threshold current and the differential efficiency had a great scatter from sample to sample. This result is quite expected because the samples were manufactured in first technological experiments with heterostructures of this type. The main goal of our experiments was to investigate the dependences of the positions and widths of the peaks on the pump current density, and these dependences did not exhibit a great scatter from sample to sample.

These data can be reduced to the dependence of the effective refractive index n_{eff} of the mode on the pump current. The value of n_{eff} is usually defined as

$$n_{\text{eff}} = \frac{\beta}{k_0}, \tag{1}$$

where $k_0 = 2\pi/\lambda = \omega/c$ is the wave vector in vacuum; β is the complex propagation constant for a waveguide mode; λ is the wavelength in vacuum; ω and c are the frequency and speed of light, respectively.

We assume that the waveguide-mode field E propagates along the z axis of the waveguide proportionally to the factor $\exp(i\beta z - i\omega t)$.

According to [3] and references therein, the angular positions θ_0 and θ_1 of the peaks in the far field of the laser (see Fig. 3) are related to the effective refractive indices $n_{\rm eff}^0$ and $n_{\rm eff}^1$:

$$n_{\rm eff} = \left(n_{\rm s}^2 - \sin^2\theta\right)^{1/2}, \tag{2}$$

where $n_{\rm eff}$ is the real values of the effective refractive indices for the zero ($n_{\rm eff}^0$) and first ($n_{\rm eff}^1$) modes; $n_{\rm s}$ is the refractive index of a substrate. The latter is commonly known with sufficiently good accuracy because the substrate is manufactured from a bulky material and its refractive index can be readily measured.

Therefore, the data in Fig. 3 unambiguously demonstrate the change in the effective refractive indices with the pump current density. (The error of measurement of the angle $\theta \sim 0.2^\circ$ corresponds to the accuracy of the measurement of the refractive index of $\sim 10^{-3}$.) This change is caused by two dominating mechanisms: a decrease in the refractive index of active layers with increasing concentration of injected carriers (pumping current) and an increase in the refractive index of the structure layers located close to the sources of heat release due to heating (increase in the current). These mechanisms have opposite effects, which are different for different layers and in different ranges of the pump current. The dependence of $\delta n_{\rm eff}$ on the concentration N of carriers can be readily found within the framework of the perturbation theory by using a standard method for determining the first-order correction from the Helmholtz equation to which the problem of finding $n_{\rm eff}$ is reduced:

$$\delta^N n_{\rm eff} = \Gamma \frac{1}{2n_{\rm eff}} \frac{\partial \varepsilon'}{\partial N} \delta N, \tag{3}$$

where Γ is the total (for all active layers) factor of the optical confinement; and ε' is the real value of the permittivity of an active layer. It is obvious that, first, this effect depends on the overlap of the mode field and the active layer (Γ factor), and for this reason it will be different for the zero and first modes. Second, the effect will be substantial only for pump below the threshold. Because the concentration N is stabilised at the lasing threshold and above, this mechanism will not contribute to the change in $n_{\rm eff}$ for currents above the threshold.

The temperature dependence of $\delta n_{\rm eff}$ can be calculated from the relation

$$\delta^T n_{\rm eff} = \frac{1}{2n_{\rm eff}} \sum_i \frac{\partial \varepsilon_i'}{\partial T} \delta T_i \Gamma_i, \tag{4}$$

where $\partial\varepsilon_i'/\partial T$ is the derivative of the real part of the permittivity of the ith layer at temperature T; δT_i is the change in the temperature of the ith layer caused by the heat release in the layer and heat transfer to it from other layers; and Γ_i is the optical confinement factor of the ith layer. Because heat release occurs at any pump current, the effective refractive index will depend on temperature both upon pumping below and above the threshold. The coefficient of conversion of the electric energy to heat changes upon passing through the lasing threshold. However, in our case, the maximum variation in this coefficient did not exceed two times (the lasing efficiency was lower than 50 %). It is known that the characteristic distance over which the heat propagates in the structure layers during the pulse of duration ~ 300 ns is of about $3-5$ μm, which exceeds a total thickness of all waveguide layers or comparable to it. Therefore, we can use relation (4) for estimates, in which the value of δT_i is the same for all the layers and also all the values of $\partial\varepsilon_i'/\partial T$ are the same and close to $\partial\varepsilon_0'/\partial T$, for which Γ is maximum. Taking this into account, we can assume that

$$\delta^T n_{\rm eff} \approx \frac{1}{2n_{\rm eff}} \frac{\partial \varepsilon_0'}{\partial T} \delta T. \tag{5}$$

It is easy to understand qualitatively the dependence of the angles θ_0 and θ_1 on the pump current (Fig. 3). For the current density $j < j_{\rm th}$, the dependence of $\delta n_{\rm eff}$ on N becomes dominant [according to (3)]. The value of N decreases with increasing $\delta n_{\rm eff}$ ($\partial\varepsilon'/\partial N < 0$). The thermal effect only somewhat slows down the change in $\delta n_{\rm eff}$. Correspondingly, the angles θ_0 and θ_1 increase with the current density. Above the lasing threshold, the change in $\delta n_{\rm eff}$ is mainly determined by the thermal mechanism. Because $\partial\varepsilon_0'/\partial T \approx 1.5 \times 10^{-3}$ $\mathrm{K}^{-1} > 0$, the increase in the current above the threshold results in the decrease in the angles θ_0 and θ_1.

The value of δT in (5) can be estimated by assuming that the heating of waveguide layers is close to adiabatic and that half the energy delivered to the laser is converted to heat. As a result, we have

$$\delta T_{\rm max} \approx \frac{1}{2} \frac{JV\tau}{C}, \tag{6}$$

where $\delta T_{\rm max}$ is the change of the temperature during the pulse; J is the total current; V is the voltage across the laser diode; $\tau = 300$ ns is the pulse duration; C is the heat capacity of layers in which the heat has been retained during the pulse. Because the temperature of waveguide layers changes almost linearly during the pulse, we can assume that $\delta T = {}^1\!/_2 \delta T_{\rm max}$ in (5). For the laser parameters presented in Fig. 3, the value of C was estimated as 3×10^{-7} J K^{-1}. In this case, the thermal variation $\mathrm{d}\theta/\mathrm{d}j$ estimated from (5) and (6) is 4×10^{-5} K cm^2 A^{-1}, while according to Fig. 3, it is equal to 5×10^{-5} K cm^2 A^{-1}. Thus, one can see that the agreement between the calculation and experiment is acceptable.

The ratio of the slopes of the dependences of θ_0 and θ_1 on the pump current density in Fig. 3 for $j < j_{\rm th}$ is ~ 1.6, which gives the estimate of the ratio of the Γ factors for the zero and first modes. To estimate Γ factors quantitatively, we used the calculation of the waveguide structure of the lasers studied. The initial data for calculations of the layers were the layer parameters, which were used as approximate in the growing of the structures. Then, to obtain the best fit with the experiment, we corrected these parameters (thickness and composition of the layers) in calculations (within the limits of the technological accuracy provided upon growing heterostructures). The calculations gave the distributions of the fields of each mode in the waveguide.

The Γ factors calculated for the zero and first modes were 1.1×10^{-2} and 0.75×10^{-2}, respectively. The value of $(\partial\varepsilon_{\rm a}'/\partial N)(\partial N/\partial j) = \partial\varepsilon_{\rm a}'/\partial j$ (where $\varepsilon_{\rm a}'$ is the real part of the permittivity of the active layer) calculated from relations (3) and (4) and the data in Fig. 3 was approximately equal to -0.9×10^{-3} cm^2 A^{-1}, which is close to the value -1.0×10^{-3} cm^2 A^{-1} found in experiments performed by the different method for other lasers with the close thickness and composition of the active region (see Fig. 3 in paper [5]).

It may appear at first glance that the presence of many free parameters for fitting the calculated values of θ_0 and θ_1 to their experimental values provides a significant freedom. However, this is not the case. This is clearly demonstrated by the difference between the preliminary specified and really obtained thickness of layers nos 4 and 10 (see Table 1). It was assumed upon growing the structure that these layers will have the same thickness, which would provide some symmetry of the layers. According to such a notion, which was confirmed by the calculation, the first mode not only could not be excited in such a structure but spontaneous radiation to this mode would be also extremely weak. This is caused by the arrangement of active layers in the waveguide parts where the amplitude of this mode was close to zero. If even some spontaneous radiation in this mode came outside, no motion of the peak would be observed in the far-field zone because the Γ factor for this mode would be close to zero.

For this reason, the experimental data obtained for the first mode can be explained only by the existence of some asymmetry of the waveguide structure, which provides the noticeable overlap of the field of the first mode with active layers, as well as a rather high values of the Γ factor, which is only 1.6 times smaller than that for the zero mode. This is a rather stringent condition, which can be satisfied by fitting not so many free parameters. In particular, this can be done by varying the thickness of layers nos 4 and 10 (see Table 1). Fig. 2b shows the typical calculated distributions of the intensity of the zero and first modes obtained by varying the layer thickness.

The change in the width of peaks in the far-field zone observed in experiments is also caused by the change in the concentration of carriers below the threshold and the change in the temperature above the threshold. According to [3], the angular width $\Delta\theta_0$ of the peak in the far-field zone is determined by the imaginary part β_x'' of the propagation constant of the inhomogeneous wave in the substrate leaking in the direction perpendicular to the layers:

$$\Delta\theta \propto \left|\beta_x''\right| \approx \frac{n_{\text{eff}}\left|\alpha - \alpha_s n_{\text{sc}}/n_{\text{eff}}\right|}{2\sin\theta}, \tag{7}$$

where $\alpha = \alpha_{\text{L}} + \alpha_{\text{sc}} - g(N)$ are total optical losses in the waveguide; α_{L} is the leaky losses; α_{sc} is the losses caused by absorption and scattering in the waveguide layers; $g(N)$ is the mode gain in active layers; α_s is optical losses in the substrate. In our case, the value of $\alpha_{\text{L}} + \alpha_{\text{sc}}$ is substantially larger than α_s, so that $\Delta\theta$ decreases in the regime below the threshold and, according to (7), vanishes near the lasing threshold when $\alpha \approx 0$. However, we should take two circumstances into account: the finite aperture of the output beam determined by the substrate thickness D and the broadening of the peak caused by the small-angle scattering from large-scale inhomogeneities in the substrate. In our case, $D = 300$ μm, giving the limiting value

$$\Delta\theta \approx \frac{\lambda}{D\cos\theta} \approx 0.2^\circ. \tag{8}$$

The minimum value of $\Delta\theta$ observed experimentally was $\sim 0.4^\circ$.

For currents above the lasing threshold, the value of α is stabilised and the concentration dependence of $\Delta\theta$ should be absent. However, we observed in experiments the stabilisation of $\Delta\theta$ at the minimum level only near the lasing threshold. As the current was further increased above the lasing threshold, the value of $\Delta\theta$ increased monotonically. This increase can be interpreted as the result of the peak movement in the far-field zone of the laser during the pump pulse.

The temperature dependence of the angle θ corresponding to the maximum in the far-field distribution was discussed above by analysing data in Fig. 3. As was mentioned, because of the adiabatic character of heating, the temperature dependence of n_{eff} will be almost linear during the pump pulse. This means that the temperature broadening $\Delta\theta$ will be close to the shift $\delta\theta$ of the angle. Indeed, the data in Fig. 4 show that when the pumping current was changed from the threshold to the maximum value, the variation in the angle was $\delta\theta \approx 1.4^\circ$, whereas the variation in $\Delta\theta$ was $\sim 1.1^\circ$. A small difference between these values can be explained by the fact that the duration of lasing at the first mode is somewhat shorter than the pump-pulse duration or by the dependence of the peak shape in the far field on the pump current. In addition, the nonlinearity of the temperature effect should be taken into account.

It is obvious that the thermal broadening exists for any pump current, including pumping below the threshold. By extrapolating $\Delta\theta$ caused by thermal broadening from the region $j \gg j_{\text{th}}$ to the region $j < j_{\text{th}}$, we find the thermal contribution to $\Delta\theta$ for $j = j_{\text{th}}$. According to the data presented in Fig. 4, this contribution is $\sim 0.2^\circ$. Therefore, the difference between the experimental value $\Delta\theta_{\min} = 0.4^\circ$ and the theoretical limit of 0.2° is substantially determined by the thermal contribution to $\Delta\theta$. This suggests that upon cw lasing, the value of $\Delta\theta$ will be close to the theoretical limit.

A rather complicated distribution of the 'mean' output power between the zero (I_0) and first (I_1) modes presented in Fig. 5 can be easily interpreted in the initial interval for currents $j < 12$ kA cm^{-2}. In this interval, lasing mainly occurs on the zero mode. As the pump current is further increased, lasing on the first mode appears. It seems that the initial difference between the mode gains is not too large and can be eliminated due to temperature variations in the waveguide properties of the active region or because of the spatially inhomogeneous (along quantum-size layers) saturation, resulting in excitation of the first mode. A more detailed analysis of the dependences of I_0 and I_1 on the pump current is beyond the scope of this paper.

4. Conclusions

We have found experimentally for the first time the shift of peaks in the far radiation field of leaky-mode lasers. It is shown that this shift is caused by the change in the effective refractive index produced by injected carriers and by the change in the temperature of waveguide layers.

We have demonstrated by the example of the lasers studied that, by using the calculations of the waveguide structure and the results of experimental studies of the radiation pattern, we can measure the important parameters of the lasers such as the effective refractive index, the optical confinement factor, and the coefficient characterising the dependence of the refractive index of the active layer on the concentration of injected carriers. The accuracy of the measurement of the effective refractive index can be as high as $\sim 10^{-3}$. All this can be used as an independent method, which supplements the known methods based, for example, on spectral measurements.

Acknowledgements. The authors thank V I Shveikin for placing laser samples at their disposal. The work was performed within the framework of the program 'Physics of Solid-State Nanostructures' and was partially supported by the Russian Federal Program 'Integration' (Grant No A055), Teaching and Research Centre 'Fundamental Optoelectronics of Quantum-Well Semiconductor Lasers', and by the Grant No. 00-15-96624 of the Advanced Scientific Schools.

References

1. Shveikin V I Bogatov A P, Drakin A E, Kurnyavko Yu V RF Inventor's Certificate no. 2134007, 12.03.1998
2. Bogatov A P, Drakin A E, Shveikin V I *Kvantovaya Elektron.* **26** 28 (1999) [*Quantum Electron.* **29** 28 (1999)]
3. Shveikin V I, Bogatov A P, Drakin A E, Kurnyavko Yu V *Kvantovaya Elektron.* **26** 33 (1999) [*Quantum Electron.* **29** 33 (1999)
4. Bogatov A P, Drakin A E, Stratonnikov A A, Konyaev V P *Kvantovaya Elektron.* **30** 401 (2000) [*Quantum Electron.* **30** 401 (2000)]
5. Bogatov A P, Boltaseva A E, Drakin A E, Belkin M A, Konyaev V P *Kvantovaya Elektron.* **30** 315 (2000) [*Quantum Electron.* **30** 315 (2000)]